Comparison of patch acoustic holography methods
for confined space

Zdeněk HAVRÁNEK[1]; Petr BENEŠ[2]; Stanislav KLUSÁČEK[3]

[1,2,3] Brno University of Technology, Czech Republic

ABSTRACT

Localization and characterization of noise and vibration sources through measurement of sound fields radiated from vibrating structures plays an important role in vibration diagnostics. Sound pressure field measured in closed distance to the source with a microphone array is then inversely processed with the suitable near-field acoustic holography method to obtain the estimation of sound field very near the identified source surface. Several restrictions apply when measurement is performed in non-anechoic conditions and with the array smaller than the examined source. In these cases patch holography methods with sound field separation technique should be used. The Equivalent Source Method (ESM), Statistically Optimized Near-field Acoustical Holography (SONAH) and iteratively enhanced Fourier transformation based procedure are examples of such methods. In this paper an extensive comparison of these source identification methods has been carried out while other disturbing sources affect the acquired data. Experimental evaluation of the methods has been performed in ideal anechoic conditions and further in disturbing environment. Real measurement data has been obtained with double layer planar rectangular microphone array with MEMS transducers and the results of principal source identification accuracy for all methods have been presented. Some practical aspects of applicability of each method are also discussed.

Keywords: acoustic holography, microphone arrays, confined space
I-INCE Classification of Subjects Number(s): 75.7, 74.7, 74.6, 72.2.2

1. INTRODUCTION

Localization and characterization of noise and vibration sources through acoustic measurement and with using specific calculation algorithms and methods for sound field estimation near the examined source surface have been continuously investigated nearly thirty years. The first foundation of the acoustic imaging of sound sources based on methods usually called near-field acoustic holography (NAH) has been laid by Williams and Maynard in early 80' (1, 2, 3). Successful utilization of general planar methods for sound source identification in nearly anechoic conditions has been extended to specific procedures intended for more practical applications where more complicated sound sources are examined. For large area sound sources and while using classical methods, estimation and reconstruction of sound field near the source surface can be successful only with measurement microphone array larger than the source. This limitation has been overcome in the last decade with several new methods using the array smaller than the radiating surface. Such perspective methods perform backward reconstruction directly in spatial domain, thus avoid spatial windowing required for classic Fourier based methods. These methods are usually called "patch" methods because only one small measured area of the sound field above its surface can be used to calculate the radiation from the source and estimation of the sound field very near the source. Popular patch holography methods developed in last years were Statistically Optimized NAH algorithm (SONAH) and method based on equivalent sources (ESM) (4, 5).

After it was proved that the patch methods are strong and robust main interest of researchers in the field of acoustic holography has moved to the applicability of these methods to estimate sound radiation from structures in the enclosures (car cabins, aircrafts, trains, etc.). Classical planar acoustic

---

holography theory (2) assumes that all sources are only on one side of the measurement (hologram) plane. If sources exist on the other side or there are some reflections of the primary (examined) source, the reconstruction of the sound field near primary source is very difficult and incorporates large errors. The sources on behind the measurement plane (on the "wrong" side) usually affects the prediction accuracy which in most cases leads to underestimation of the sound field radiated from primary source.

This situation expects separation of incoming and outgoing sound field at the measurement location, thus requires that measurement should be performed not only in two dimensional area (e.g. with planar array), but uses three-dimensional arrays with acoustic sensors mounted in two layers, for planar holography, or on the sphere, for spherical holography. Already mentioned holography algorithms as SONAH and ESM are suitable for measurement with microphones in two parallel planes and reconstruction of sound field near the source in confined space (4, 6, 8).

Another possibility to enhance the reconstruction accuracy of the NAH algorithms is to use velocity transducers instead of pressure transducers (microphones) for measurement of the sound field. This leads to less regularization of the inverse procedure which is always somehow necessary (7). Also combination of pressure and particle velocity probes has been successfully tested to improve reconstruction accuracy in practical applications (7, 10).

This paper describes both simulation and experimental study where three different patch acoustic holography methods have examined and results of sound source localization has been compared. All of the methods can use the information of the sound field measured in two parallel planes above the examined source and for this purpose the measurement apparatus should have two layers of pressure sensors. Our experiments have been carried out with commercial MEMS microphones to show the applicability and usability of the tested methods. Two of the selected methods are pure patch holography methods – SONAH and ESM, thus examined source can be larger than the array, and the last one can be used in confined space, but there are several restrictions on the applicability as a patch method, because uses Fourier transformation and affects resulting hologram specially on its edges. To minimize the truncation effect in the classical procedure with Fourier transformation, an iterative procedure with Wiener filter has been supplemented (9).

There are also other patch holography methods applicable in confined space, but their usability with planar microphone array and nearly planar source surface is not very suitable because they use different sound field model, e.g. Helmholtz Equation Least Squares (HELS) method (11), which uses spherical wave functions to describe the sound field near the examined source and Inverse Boundary Element Method (IBEM), which is more applicable and useful for more arbitrary geometries and is also more computational intensive.

2. PATCH HOLOGRAPHY METHODS

In the next paragraphs there will be given a basic and very general description of the philosophy and mathematical foundation of the three patch holography methods applicable in confined space, thus successful in the environments where other disturbing sources and reflections are present.

All three methods have been selected based on the criteria to use them for acoustic imagining of sources generated by planar radiators (e.g. thin plates, nearly planar structures) and using double layer planar matrix microphone array as a measuring device providing necessary input data. In this selection we also exclude the methods which are element based thus computationally intensive.

2.1 Equivalent source method

Basic theory of the equivalent source method (ESM) is based on the idea that sound field above the vibrating structure can be modeled by several number of simple sources placed in the structure closed to the radiating surface. So this method is generally using superposition. If there are M measurement points on the hologram plane and N equivalent sources placed in the structure, the sound pressure vector p_{h1} measured with microphones in one plane can be expressed in matrix form as (7):

$$\mathbf{p}_{h1} = j\rho ck\mathbf{G}_1\mathbf{W}_1 \qquad (1)$$

where ρ is the density of the medium, c is the speed of sound, k is the wave number and W_1 is the column vector containing the strengths $w_{11}(\mathbf{r}_{o1})$, $w_{12}(\mathbf{r}_{o2})$, .. $w_{1n}(\mathbf{r}_{on})$ of the equivalent sources, $\mathbf{r}_{on}$ is the nth equivalent source location vector, and G_1 is the transfer matrix between equivalent sources and the measurement points. This transfer matrix contains Green's functions between all source and measurement points is defined as:

$$\mathbf{G}_1 = g\left(\mathbf{r}_{hm} - \mathbf{r}_{sn}\right) = -\frac{\mathrm{e}^{ikr}}{4\pi r}, \quad r = \left|\mathbf{r}_{hm} - \mathbf{r}_{sn}\right|. \tag{2}$$

While sound field separation is necessary, two measurement surfaces p_{h1} and p_{h2} are needed and also two fictitious surfaces S_1 and S_2 with the redistributed equivalent sources are necessary. Then for the incoming (superscript "i") and outgoing (superscript "o") sound field measured on hologram planes, several matrix equations can be written based on both equivalent sources strengths. Both directions of pressure field for the first hologram plane (closed to the examined source S_1) can be expressed as:

$$\mathbf{p}_{h1} = \mathbf{p}_{h1}^{i} + \mathbf{p}_{h1}^{o}, \quad \mathbf{p}_{h1}^{o} = \mathbf{G}_1^{o} \mathbf{W}_1, \quad \mathbf{p}_{h1}^{i} = \mathbf{G}_1^{i} \mathbf{W}_2. \tag{3}$$

Similarly on the second (rear) hologram plane:

$$\mathbf{p}_{h2} = \mathbf{p}_{h2}^{i} + \mathbf{p}_{h2}^{o}, \quad \mathbf{p}_{h2}^{o} = \mathbf{G}_2^{o} \mathbf{W}_1, \quad \mathbf{p}_{h2}^{i} = \mathbf{G}_2^{i} \mathbf{W}_2. \tag{4}$$

To evaluate the source strengths vectors $\mathbf{W}_1$ and $\mathbf{W}_2$, the above equations 3 and 4 can be rewritten to equations 5 and 6.

$$\mathbf{W}_1 = \left(\mathbf{G}_1^{o} - \mathbf{Q}_1 \mathbf{G}_2^{o}\right)^{\dagger} \left(\mathbf{p}_{h1} - \mathbf{Q}_1 \mathbf{p}_{h2}\right), \quad \mathbf{W}_2 = \left(\mathbf{G}_2^{i} - \mathbf{Q}_2 \mathbf{G}_1^{i}\right)^{\dagger} \left(\mathbf{p}_{h2} - \mathbf{Q}_2 \mathbf{p}_{h1}\right), \tag{5}$$

where

$$\mathbf{Q}_1 = \mathbf{G}_1^{i} \left(\mathbf{G}_2^{i}\right)^{\dagger}, \quad \mathbf{Q}_2 = \mathbf{G}_2^{o} \left(\mathbf{G}_1^{o}\right)^{\dagger}. \tag{6}$$

Inversions of the transfer matrices (with superscript "†") is obtained from their origins by singular value decomposition and afterwards the source strengths vectors can be calculated. This operation is the last step of the sound field separation only if the surface of the S_1 is totally absorbing (no scattered field of the second source S_2 is produced on the examined surface). If there is some reflection from the source surface and scattered field is present, one more calculation step is needed. In case when the examined surface is totally reflecting, the scattered field can be expressed in matrix form:

$$\mathbf{p}_{h1}^{s} = \mathbf{G}_{1s}^{o} \mathbf{W}_2, \tag{7}$$

where G_{1s} is the transformation matrix for scattering (only for this simple case as total reflection) and can be calculated as transfer matrix of the mirror source of S_2, placed behind the examined surface (in the source S_1 region), to the first hologram plane. Finally the "free-field" radiated part of the sound pressure measured at the first hologram plane can be expressed in matrix form with equation:

$$\mathbf{p}_{h1}^{f} = \mathbf{p}_{h1}^{o} - \mathbf{p}_{h1}^{s} = \mathbf{G}_1^{o} \mathbf{W}_1 - \mathbf{G}_{1s}^{o} \mathbf{W}_2. \tag{8}$$

When the contribution only from examined source is known the last inverse calculation of transfer matrix $\mathbf{G}_1^{f}$ is needed to obtain an estimation of equivalent source strengths $\mathbf{W}_f$ representing radiation produced only by the examined source. In matrix form the last statement is written as:

$$\mathbf{p}_{h1}^{f} = \mathbf{G}_1^{f} \mathbf{W}_f. \tag{9}$$

If the equivalent source strength $\mathbf{W}_f$ for „free-field" radiation of the examined source is estimated, sound pressure at any point above the source can be calculated. From the complete derivation of ESM for patch measurement in confined space it can be easily demonstrated that the method is also suitable for irregular geometries of the hologram „plane" and the examined source surface.

2.2 Statistically Optimized NAH

Second popular and robust patch holography algorithm is Statistically Optimized Near-field Acoustic Holography (SONAH) and also calculates forward or backward propagation directly in the spatial domain without involving spatial DFT. Generally, SONAH procedure assumes that there can be find such set of elementary plane wave functions Ψ_n, $n = 1,2,..N,$ that can describe the complete sound field near the examined source:

$$\Psi_n\left(\mathbf{r}\right) = \kappa \Phi_{\mathbf{k}_n} \equiv \kappa F_n\left(k_z\right)e^{j(k_x x + k_y y + k_z z)}, \tag{10}$$

where κ is a scaling factor supporting smooth transition for continuous wave spectra, while there are regular sampling in the wave number domain, and F_n are amplitude weighting functions with the unit weighting at the virtual source plane.

Complex estimation weights $\mathbf{c}(\mathbf{r})$ between a set $\mathbf{A}$ of elementary wave functions representing the sound field at the hologram plane and a set $\boldsymbol{\alpha}(\mathbf{r})$ representing the sound field at an estimation position can be written in matrix form as $\mathbf{Ac}(\mathbf{r}) = \boldsymbol{\alpha}(\mathbf{r})$ and Tikhonov regularized solution for $\mathbf{c}(\mathbf{r})$ can be expressed as:

$$\mathbf{c}(\mathbf{r}) = \left(\mathbf{A}^H \mathbf{A} + \varepsilon \mathbf{I}\right)^{-1} \mathbf{A}^H \boldsymbol{\alpha}(\mathbf{r}), \tag{11}$$

where ε is a regularization parameter, $\mathbf{I}$ is a diagonal unity matrix and $\mathbf{A}^H\mathbf{A}$ is the cross correlation matrix between the measurement points in the domain of elementary wave functions and similarly vector $\mathbf{A}^H\boldsymbol{\alpha}(\mathbf{r})$ contains cross correlation between the measurement points and the estimation position $\mathbf{r}$. Both cross correlation equations is written below.

$$\left[\mathbf{A}^H\mathbf{A}\right]_{ij} = \sum_n \Psi_n^*(\mathbf{r}_i)\Psi_n(\mathbf{r}_j) = \frac{1}{2\pi k^2} \int_{-\infty}^{\infty}\int_{-\infty}^{\infty} \Phi_{\mathbf{k}}^*(\mathbf{r}_i)\Phi_{\mathbf{k}}(\mathbf{r}_j)dk_x dk_y \tag{12}$$

$$\left[\mathbf{A}^H\boldsymbol{\alpha}(\mathbf{r})\right]_{ij} = \sum_n \Psi_n^*(\mathbf{r}_i)\Psi_n(\mathbf{r}) = \frac{1}{2\pi k^2} \int_{-\infty}^{\infty}\int_{-\infty}^{\infty} \Phi_{\mathbf{k}}^*(\mathbf{r}_i)\Phi_{\mathbf{k}}(\mathbf{r})dk_x dk_y \tag{13}$$

When the complex coefficient vector $\mathbf{c}(\mathbf{r})$ is calculated, sound pressure at any point in the source-free region can be estimated by linear combination of known sound pressure values $\mathbf{p}$.

$$p(\mathbf{r}) = \mathbf{p}^T \mathbf{c}(\mathbf{r}), \tag{14}$$

The above derivation of pressure reconstruction with sound source at only one side of the hologram plane can be extended for situation where there are sources on both sides. This leads to adding corresponding set of plane wave functions related to the second virtual source plane to the cross correlation matrix $\mathbf{A}^H\mathbf{A}$ and vector $\mathbf{A}^H\boldsymbol{\alpha}(\mathbf{r})$. Detailed definition of reconstruction in non free-field conditions can be found in (4).

2.3   NAH with Fourier transformation

Last method under investigation was classical planar holography algorithm based on 2D spatial Fourier transformation but supplemented with separation task and enhanced with recursive iterative technique in wave-number domain to minimize the effect of spatial windowing and wavenumber filtration to allow usage of such general algorithm as a patch method and in a confined space.

Based on general equation of transformation of sound fields in wavenumber domain, the backward prediction of sound pressure image $\mathbf{P}_h$ at the hologram plane to the estimation plane $\mathbf{P}_x$ is governed by simple inverse propagator $\mathbf{G}_{pi}$ (Green's function) and k-space filter $\mathbf{K}_f$ as defined by equation:

$$\mathbf{P}_x = \mathbf{P}_h \mathbf{G}_{pi} \mathbf{K}_f. \tag{15}$$

To be able to separate incoming and outgoing sound field and calculate only contribution from the examined source at the first hologram plane $\mathbf{P}_h$, separation term defined in wavenumber domain by equation 16 can be used (9).

$$\mathbf{P}_h = \frac{\mathbf{P}_{h1} - \mathbf{P}_{zh2}e^{ik_z D}}{1 - e^{i2k_z D}}. \tag{16}$$

Where $\mathbf{P}_{h1}$ is the wavenumber spectrum of the sound pressure in the first plane, $\mathbf{P}_{h2}$ is similarly the spectrum in the second plane and D is the separation distance between the planes.

The separation term expects information about sound field in two parallel planes thus requires measurement of sound pressure with double layer array technique. The above mentioned separation term has been proved to be able to separate the wave components coming from the two sides of the array (9). This denominator of the term is ill-conditioned for wavenumber components near the radiation circle thus requiring some smoothing of radiation circle by integration of k_z over the small

region in wavenumber domain.

Finally to improve prediction accuracy of the algorithm and minimize the influence of the spatial windowing and wavenumber filtration to estimated sound pressure field near the examined source recursive iterative method based on Wiener filter is used. The recursive algorithm starts with the first estimation of sound pressure spectra $\mathbf{P}_{x0}$ where uses simple propagation as defined by equation 15 and in next iterations new estimation of sound pressure spectra at calculation plane is determined with equation 17, where $\mathbf{G}_p$ represents forward propagator, superscript "i" at calculated spectra denotes iteration number and ε is the regularization parameter.

$$\mathbf{P}_x^i = \mathbf{P}_x^{i-1} + \mathbf{W}\left(\mathbf{P}_h - \mathbf{G}_p \mathbf{P}_x^{i-1}\right), \quad \mathbf{W} = \frac{\mathbf{G}_p^*}{\left|\mathbf{G}_p\right|^2 + \varepsilon^2}. \tag{17}$$

The regularization incorporated in the Wiener filter reduces high spatial frequencies and thus exponential amplification of evanescent wave and also ensures the convergence of the algorithm in presence of noise in the measured data. It is advisable that the procedure using measurements in two parallel planes is also supplemented with enlargement of the holograms' apertures by zero padding. For this iterative double layer method an acronym DL-NAH will be later used in the text.

3. REFERENCE SOUND SOURCE

As a reference sound source for comparison of all selected methods, a thin plate driven by harmonic point force has been considered to produce surface vibrations which consequently generates the sound field above the plate. The plate has been considered as unclamped, so all boundaries were free and the driving force was placed very near to the one corner to ensure the excitation of the several fundamental modes. To be able to evaluate NAH algorithms on the relevant data measureable with the particular microphone array the modes have to lie in the frequency range from 250 Hz up to 5 kHz.

The reference plate has been made from aluminum alloy with dimensions of 80x25cm^2 and thickness of 2 mm. Particular eigenfrequency has been analyzed by simulations with finite element modelling software COMSOL Multiphysics and later evaluated by practical measurements with scanning laser vibrometer and vibration shaker as a driving force generator.

Experimental setup for determination of surface velocities on the plate driven with B&K vibration exciter and PXI measurement system with Polytec scanning laser vibrometer is on the figure 1.
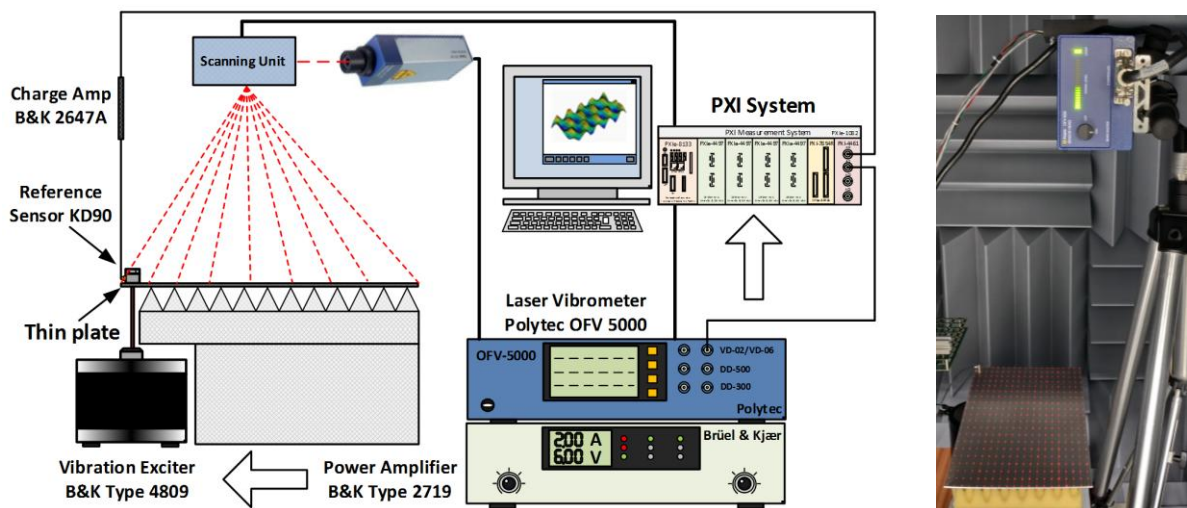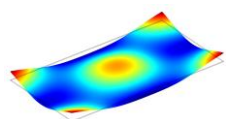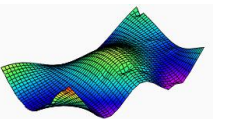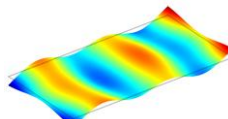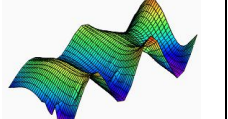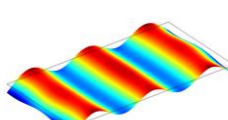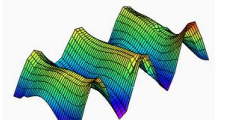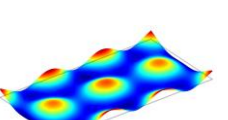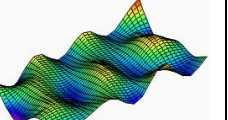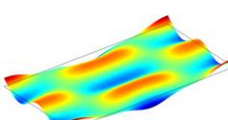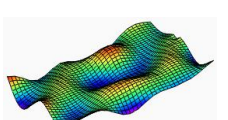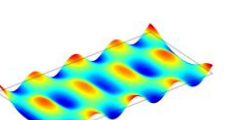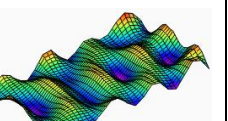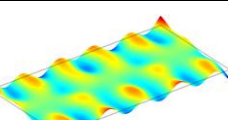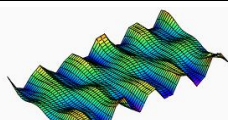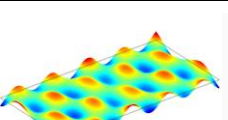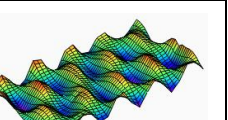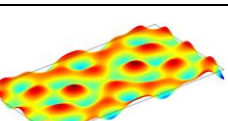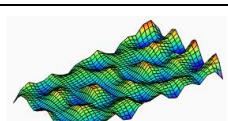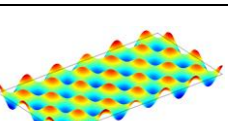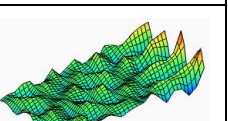

Figure 1 – Sketch and photo of the measurement setup to obtain surface velocities on the thin plate

The plate has been driven with the exciter to generate surface vibration velocity of 1 mm/s at the reference point where reference accelerometer has been placed. This reference sensor ensures the correct measurement of the relative phase during point-to-pint scanning. Surface velocities were measured in the 20x20 point grid to cover whole plate with enough accuracy for high order modes. Selected natural frequencies of the aluminum plate suitable for further testing of NAH algorithms are summarized in the table 1, where there are modal shapes obtained with finite element simulation and

also measured with scanning vibrometer system. It can be seen that measured mode shapes clearly correspond to the simulated ones especially at low frequencies where the density of the scanning grid of the laser vibrometer is sufficient.

Table 1 – Selected natural modes of the plate

f	Simulated	Measured	f	Simulated	Measured
256 Hz			395 Hz		
620 Hz			882 Hz		
998 Hz			1424 Hz		
1938 Hz			2136 Hz		
3059 Hz			4127 Hz		

At high frequencies there was considerable influence of underlay plastic foam material which damped the plate and shifts the natural frequency lower compared to the simulations and also reduces the quality of the resonance, as can be seen on mode with frequency of 4127 Hz, where the vibrations of the part of the plate which lies outside the underlay material have noticeably higher amplitudes.

Surface velocities for selected natural modes of the plate measured with laser vibrometer have been later used to calculate "true" sound fields at hologram planes and at calculation plane to be able to evaluate the accuracy of the prediction.

4. NUMERICAL SIMULATIONS

The performance of the selected algorithms have been firstly examined on simulated sound pressure data calculated from measured real surface velocities on the plate. The simulation case has the same setup parameters as practical measurement performed later to easily compare the results and to provide nearly same initial conditions.

Two acoustic measurement planes have been virtually placed above the surface of the thin plate at a distance of 35 mm and 65 mm respectively. Both measurement grids were composed of 8 x 8 points in matrix with the spacing between adjacent points (row and column) of 30 mm. The calculation plane has been considered very near the source surface to clearly visualize the sound field related to surface vibrations. To avoid excessive reconstruction errors which arise with prediction "on the surface" where the solution is hardly regularizable the distance between fictitious calculation plane and the source surface has been chosen to 10 mm. All pressure values in the field have been calculated using a numerical approximation to Rayleigh's integral.

On the figure 2 there is a surface plot of the velocity distribution on the plate and corresponding radiated field near its surface, both for 620 Hz. In the pressure surface plot, there were marked the x, y position of the calculation and hologram planes with the black rectangle covering the central part of the plate.
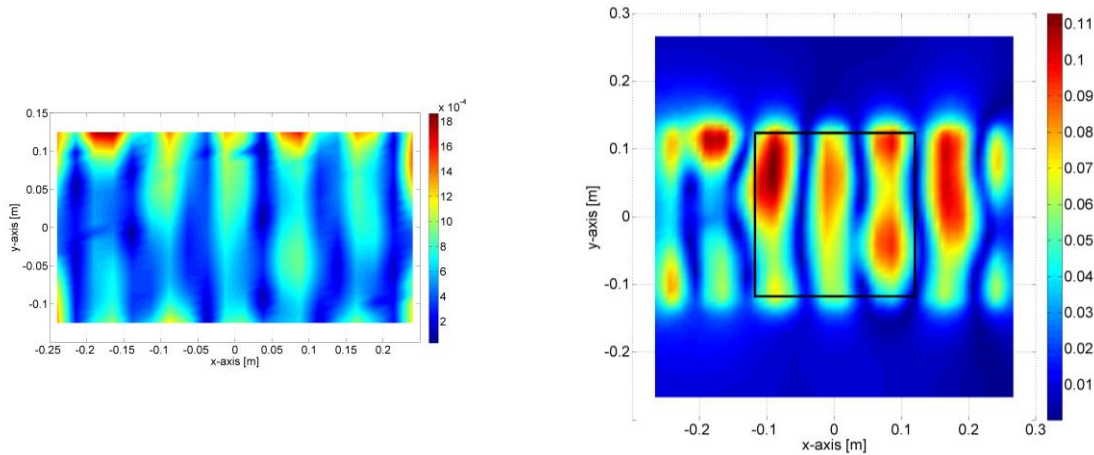
Figure 2 – Vibration velocity on the surface (left, m/s) and "true" sound pressure field on the reconstruction

plane at 10 mm distance from the source (right, Pa) for excitation frequency 620 Hz

To evaluate the reconstruction error, equation 18 representing the total error in dB on the whole calculation plane with respect to "true" values obtained by direct calculation without any disturbing sources or imperfections in the measurement chain has been used.

$$E_p = \sqrt{\frac{\left(\left|\mathbf{p}_x^{True}\right| - \left|\mathbf{p}_x^{Estimated}\right|\right)^2}{\sum_i \left|p_x^{True}\right|}} \tag{18}$$

In the first simulation case, there was only radiation from the examined source present and some amount of uncorrelated noise has been added to the measured pressure values to represent typical SNR value in input data. This simulation case thus show overall general comparison of all selected double layer algorithms and their single layer variants for simple test case where only one source is present. For ESM algorithm the equivalent sources were distributed on plane 1 cm behind the source surface and similarly the position of the virtual source plane for SONAH algorithm. For iterative DL-NAH with spatial transformations, number of iterations has been set to 500 and initial set of k-space filter were 0.4 of highest wavenumber in the spectra. All algorithms incorporate regularization parameter and for the most cases it has been selected on the estimated amount of noise included in the input data. On the figure 3 there are comparison of pressure prediction accuracy o above mentioned NAH algorithms represented by error norm E_p in decibels for SNR of 20 dB and 30 dB.
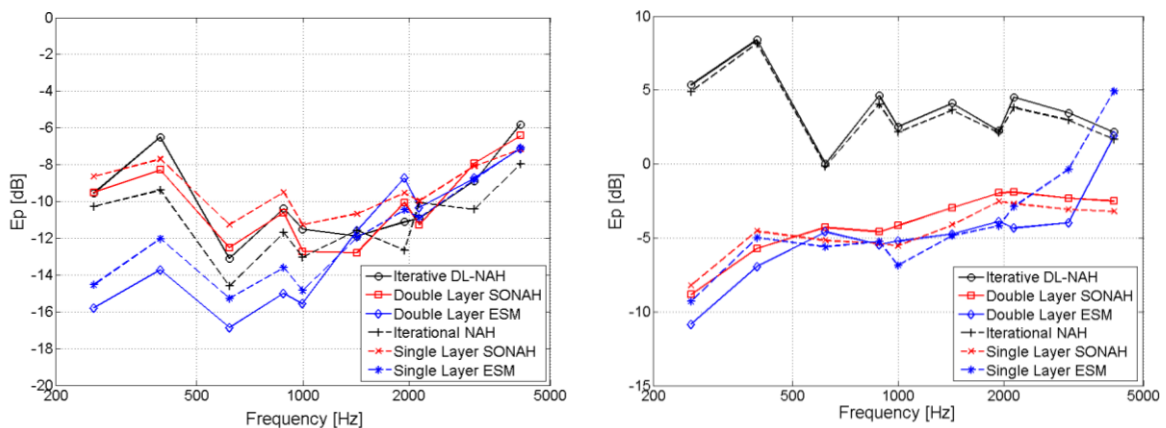

Figure 3 – Simulated pressure prediction error of single and double layer ESM, SONAH and iterative NAH

where only primary source is present and for two SNRs: 40 dB (left), 20 dB (right)

The second simulation case represents more complex sound field composed of the primary (examined) source and also from the second (disturbing) source placed on the opposite side in a distance of 350 mm from the examined source surface, thus in quite larger distance from the

measurement planes than the primary source. The strength of the second source is in similar level as the primary source and acts as a point source. Comparison of pressure prediction error in this test case for all algorithms is presented on the figure 4 also with two amount of added noise into measured data.
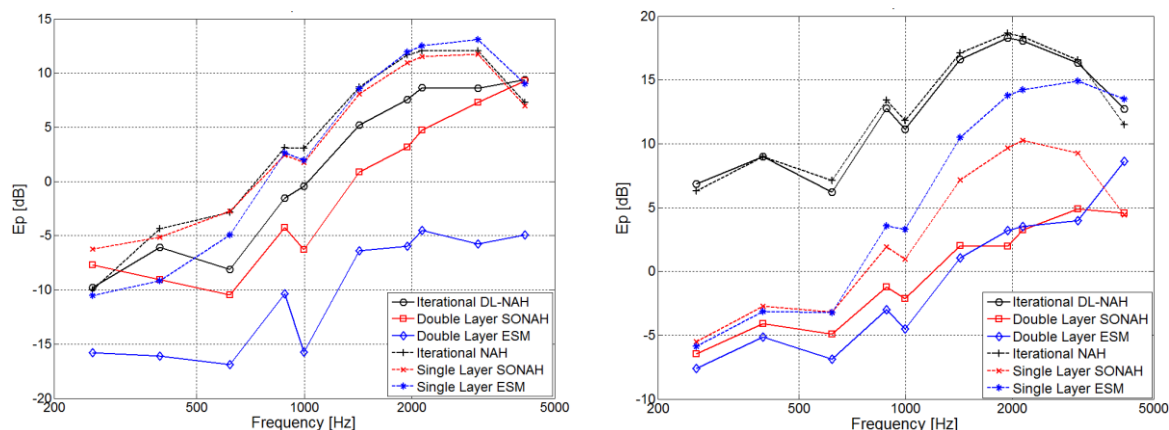

Figure 4 – Simulated pressure prediction error of single and double layer ESM, SONAH and iterative NAH

with the secondary disturbing source present with two SNRs: 40 dB (left), 20 dB (right)

5. EXPERIMENTAL SETUP AND INSTRUMENTATION

For practical evaluation of prediction performance of the selected NAH algorithms the thin plate has been installed in the small anechoic chamber with volume of approx. 10 m^3 and satisfies free-field conditions from 250 Hz. The plate was driven by the vibration exciter B&K4809 with the same strength as for the surface vibrations measurements. Pressure measurement has been carried out in two parallel planes with double layer array containing miniature commercial MEMS microphones SPM143HM4H with digital PDM output manufactured by Knowles.

Digital signal processing of data from 128 microphones has been performed in real-time on National Instruments PXI system equipped with reconfigurable FPGA digital card PXI-7854R. The radiated sound field radiated from the plate can be later disturbed with the secondary source which was represented by a loudspeaker mounted above the plate in the same distance as the virtually generated second source during the simulations (350 mm). The microphone array has been calibrated before the measurement in only very general way, so only significant phase shifts and sensitivity mismatches have been corrected. Photography and composition of the measurement setup is on the figure 5. On the next figure there is a detail of the microphone array with MEMS pressure sensors and a view of the PXI acquisition system from National Instruments where all digital signal processing has been performed and programmed mainly in LabVIEW environment.
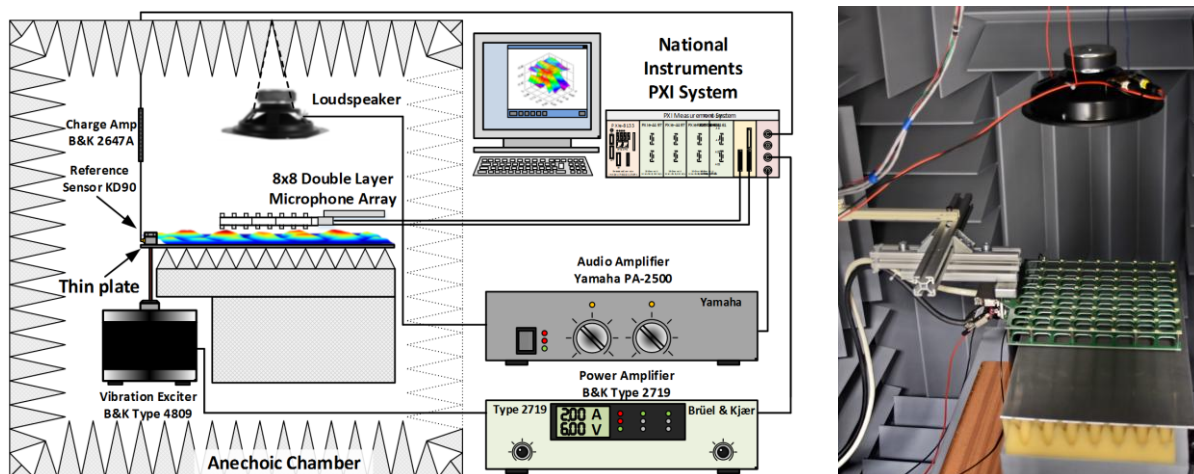

Figure 5 – Sketch and photo of the measurement setup for testing NAH algorithms on real primary source

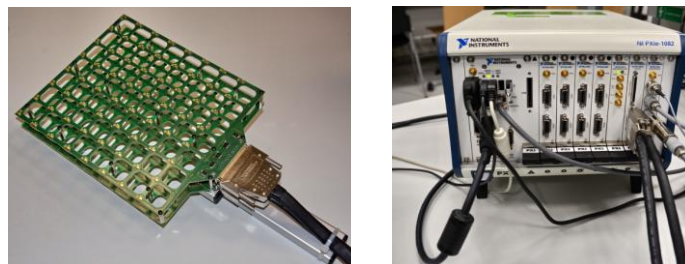(thin plate) and alternatively supplemented with secondary source (loudspeaker)

Figure 6 – Double layer array with MEMS microphones in 8x8 matrix (left) and PXI system with

NI PXI-7854 FPGA digital card (right)

6. EXPERIMENTAL RESULTS

Pressure prediction errors of the algorithms have been evaluated based on knowledge of "true" pressure which was calculated previously from the surface vibration velocities obtained with laser vibrometer measurements. In the first case only primary source was generating the sound field and afterwards also the secondary (disturbing) source has been switched on. On the left graph on the figure 7 it can be seen that without disturbing sound field all algorithms performs similarly and the reconstruction accuracy is within some region. Only iterative NAH algorithm (single or double layer) performs significantly better at higher frequencies above 1 kHz than SONAH and ESM based algorithms. If the secondary source is radiating the field to the measurement area, pressure prediction accuracy, which can be seen on the right part of the figure 7, is lower and unexpectedly all algorithms performs worse especially at low frequencies.
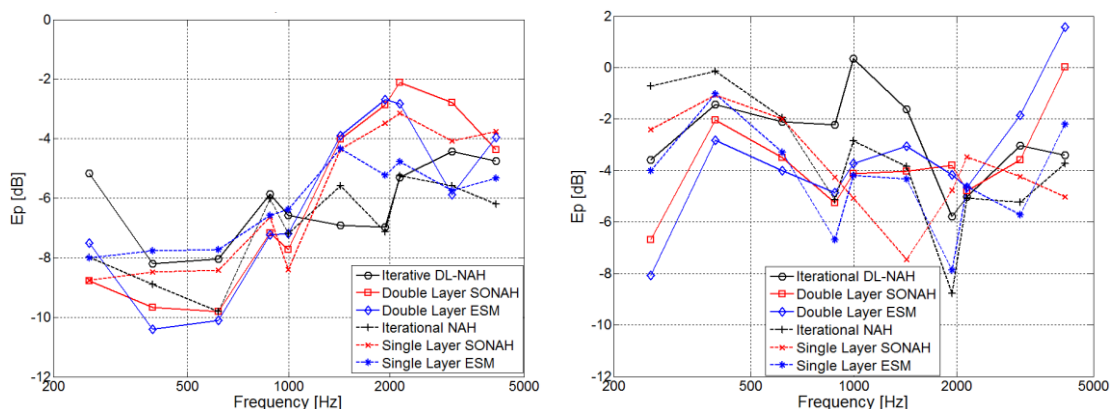

Figure 7 –Pressure prediction error of single and double layer ESM, SONAH and iterative NAH for only

primary source (left) and with the secondary disturbing source present (right)
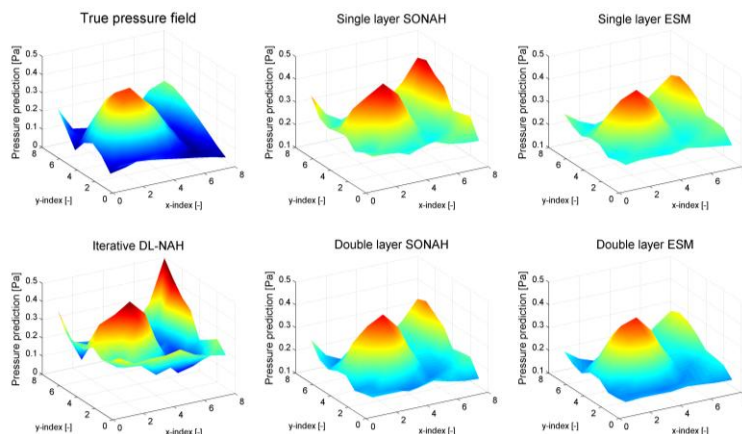

Figure 8 –Predicted pressure values obtained with different NAH methods while there are secondary

(disturbing) sound source present in the system, for frequency 256 Hz

7. CONCLUSION

Three prospecive patch NAH methods applicable in confined space has been extensively compared on simulated and also real measured data. Pressure prediction accuracy with simulated measured pressures with added amount of noise shows that single and dual layer algorithms work similarly while there is only one sound source creating measured sound field. Methods avoiding spatial tansformations are generaly less sensitive to the added noise compared to DL-NAH where the accuracy is strongly affected with the higher amount of noise in the input data even with correct level of regularization.

As can be seen also from the numerical simulations, all double layer algorithms can distiquish between incomming and outgoing sound fields, but with higher amount of noise present in the input data, DL-NAH method and SONAH algorithm are more sensitive to this type of disturbances and their prediction perfomance decreases more rapidly than NAH method based on equivalent sources. For all simulated test cases the ESM method was the most accurate prediction method.

In practical measurements all algorithms performs very similarly with only one source present, but if there is another source disturbing the measured sound field the prediction accuracy is not expectedly better with double layer methods, but consistently all methods predict sound field with much worse accuracy. This can be caused by higher number of evanescent components of the second source affecting the measured pressure field and also higher sensitivity to transducer mismatch can lead to this kind of errors. While used MEMS array has not been precisely calibrated in amplitude and phase, all these errors could lead to inability to distinguish between incoming and outgoing sound field. This behavior should be investigated in more detail in the future experiments including sensor calibration.

If we compare calculation speed of all algorithms, the slowest algorithm is SONAH, where more complicated calculations of Bessel functions is involved thus requires more time to calculate.

ACKNOWLEDGEMENTS

REFERENCES

1. Maynard, J.D., Williams, E.G. and Lee, Y. Near-field acoustical holography I. Theory of generalized holography and the development of NAH. J. Acoust. Soc. Am. 1985;78(4):1395-1413.
2. Williams, E.G. Fourier Acoustics: Sound radiation and Near-field Acoustical Holography. USA: Academic Press, 1999.
3. Williams, E.G., Maynard, J.D. Numerical evaluation of the Rayleigh integral for planar radiators using the FFT. J. Acoust. Soc. Am. 1982; 72 ():2020-2030.
4. Hald J. Basic theory and properties of statistically optimized near-field acoustical holography. J. Acoust. Soc. Am. 2009; 125(4):2105-2120.
5. Pinho M., Arruda J. On The Use of the Equivalent Source Method for Nearfield Acoustic Holography, ABCM Symposium Series in Mechatronics, Vol. 1, pp. 590-599, 2004.
6. Bi, C.-X., Chen, X.-Z., Chen, J. Sound field separation technique based on equivalent source method and its application in nearfield acoustic holography. J. Acoust. Soc. Am. 2008;123(3):1472–1478.
7. Zhang Y.-B., Jacobsen F., Bi C.-X., Chen X.-Z. Near field acoustic holography based on the equivalent source method and pressure-velocity transducers. J. Acoust. Soc. Am. 2009;126(3):1257-1263.
8. Bi, C.-X., Bolton, J.S. An equivalent source technique for recovering the free sound field in a noisy environment. J. Acoust. Soc. Am. 2012;131(2):1260-1270.
9. Havránek Z., Jacobsen F. Near-field acoustic holography with double layer array processing. In Proceedings of Euronoise 2006, pp. 1–6, Tampere, Finland, 2006.
10. Fernandez-Grande, E., Jacobsen, F., Leclère, Q. Sound field separation with sound pressure and particle velocity measurements. J. Acoust. Soc. Am. 2012;132(6):3818-3825.
11. Wu S. F. On reconstruction of acoustic pressure fields using the Helmholtz equation least squares method. J. Acoust. Soc. Am. 2000; 107(5): 2511–2522.
12. Valdivia N., Williams E. G. Approximations of inverse boundary element methods with partial measurements of the pressure field. J. Acoust. Soc. Am. 2008; 123(1):109–120.